Forebrain GABAergic Projections From the Dorsal Raphe Nucleus Identified by Using GAD67–GFP Knock-In Mice

Sun Jung Bang,[1,2] and Kathryn G. Commons[1,2]*

[1]Department of Anesthesiology, Perioperative, and Pain Medicine, Children's Hospital Boston, Boston, Massachusetts 02115
[2]Department of Anaesthesia, Harvard Medical School, Boston, Massachusetts 02115

ABSTRACT

The dorsal raphe nucleus (DR) contains serotonergic (5-HT) neurons that project widely throughout the forebrain. These forebrain regions also receive innervation from non–5-HT neurons in the DR. One of the main groups of non–5-HT neurons in the DR is γ-aminobutyric acid (GABA)ergic, but their projections are poorly understood due to the difficulty of labeling these neurons immunohistochemically. To identify GABAergic projection neurons within the DR in the current study, we used a knock-in mouse line in which expression of green fluorescent protein (GFP) is controlled by the glutamic acid decarboxylase (GAD)67 promotor. Projections of GAD67–GFP neurons to the prefrontal cortex (PFC), nucleus accumbens (NAC), and lateral hypothalamus (LH) were evaluated by using retrograde tract tracing. The location of GAD67–GFP neurons projecting to each of these areas was mapped by rostrocaudal and dorsoventral location within the DR. Overall, 16% of DR neurons projecting to either the PFC or NAC were identified as GAD67–GFP neurons. GAD67–GFP neurons projecting to the PFC were most commonly found ventrally, in the rostral two-thirds of the DR. NAC-projecting GAD67–GFP neurons had an overlapping distribution that extended dorsally. GAD67–GFP neurons made a larger contribution to the projection of the DR to the LH, accounting for 36% of retrogradely labeled neurons, and were widespread throughout the DR. The current data indicate that DR GABAergic neurons not only may have the capacity to influence local network activity, but also make a notable contribution to DR output to multiple forebrain targets. J. Comp. Neurol. 520:4157–4167, 2012.

INDEXING TERMS: tract tracing; GAD67–GFP; prefrontal cortex; nucleus accumbens; lateral hypothalamus; Fluoro-gold; periaqueductal gray

The dorsal raphe nucleus (DR), a part of the ventral periaqueductal gray, is known to be a main source of forebrain serotonin (5-HT), whose dysregulation has been associated with a variety of neuropathologies including anxiety, depression, schizophrenia, and obsessive–compulsive disorder (Neumeister et al., 2004; Hensler, 2006; Ansorge et al., 2007). Serotonergic neurons within the DR project extensively throughout the central nervous system. The ascending tracts are complex, but topographically organized such that different forebrain regions are innervated by 5-HT neurons that preferentially populate distinct regions within the DR (for review, see Vasudeva et al., 2011; Waselus et al., 2011). The topographic projection patterns of 5-HT neurons indicate that the regulation of 5-HT release in the forebrain regions is likely to be controlled by distinct groups of 5-HT neurons in the DR.

The DR also contains nonserotonergic neurons that comprise about 50–75% of the neuronal population within the DR (Moore, 1981; Descarries et al., 1982), and some of these neurons are also known to project to forebrain regions. Using rats with their 5-HT neurons chemically lesioned, a recent anterograde tract-tracing study reported dense innervation of non-5-HT neurons into the extended amygdala and basal forebrain including the lateral hypothalamus (Halberstadt and Balaban, 2008). Two major groups of non–5-HT neurons in the DR are

Grant sponsor: National Institutes of Health; Grant number: DA021801.

*CORRESPONDENCE TO: Kathryn G. Commons, Ph.D., Children's Hospital Boston, 300 Longwood Avenue, Enders 308, Boston, MA 02115. E-mail: kathryn.commons@childrens.harvard.edu

Received March 27, 2012; Revised April 30, 2012; Accepted May 9, 2012
DOI 10.1002/cne.23146
Published online May 17, 2012 in Wiley Online Library (wileyonlinelibrary.com)

glutamate- or γ-aminobutyric acid (GABA)-producing neurons (Descarries et al., 1982; Brown et al., 2008; Fu et al., 2010; Soiza-Reilly and Commons, 2011a,b). By using both anterograde and retrograde tract tracing, Hioki et al. (2010) demonstrated projections from vesicular glutamate transporter 3 (VGLUT3)-expressing non-5-HT neurons to the ventral tegmental area, substantia nigra pars compacta, hypothalamic nuclei, and preoptic area. Also, a fast, glutamatergic regulation of the hippocampus from the median raphe nucleus has been demonstrated (Varga et al., 2009).

Electrophysiological evidence has suggested a direct GABAergic projection from the DR to the prefrontal cortex (PFC) (Puig et al., 2005), yet the contribution of GABA neurons to forebrain projections remains poorly understood. In an attempt to improve the visualization of GABA neurons in this study, we used a mouse line in which green fluorescent protein (GFP) is knocked into the GAD67 locus to specifically identify GABAergic neurons (Tamamaki et al., 2003; Chen et al., 2010). Using this mouse line, we examined the projections of GABA neurons in the DR to three forebrain regions: the PFC, nucleus accumbens (NAC), and lateral hypothalamus (LH). The three regions were selected because they are known to receive moderate to dense innervation from neurons in the DR (Vertes, 1991) including non–5-HT neurons (Puig et al., 2005; Halberstadt and Balaban, 2008). A retrograde tract tracer, Fluoro-gold (FG), was locally injected into one of the three forebrain target regions, and the topographical organization of GAD67–GFP neurons in the DR projecting to the target regions were mapped by combining immunolabeling for GFP and FG.

Abbreviations

Am	amygdala
Cg1	cingulate cortex
CPu	caudate putamen
DR	Dorsal raphe
DR-C	Caudal dorsal raphe
DR-MD	Mid-dorsal subdivision of the dorsal raphe
DR-Mmlf	Medial longitudinal fasciculus at the mid-level of the dorsal raphe
DR-MV	Mid-ventral subdivision of the dorsal raphe
DR-RD	Rostral dorsal subdivision of the dorsal raphe
DR-Rmlf	Medial longitudinal fasciculus at the rostral level of the dorsal raphe
DR-RV	Rostral ventral subdivision of the dorsal raphe
DTN	Dorsal tegmental nuclei of Gudden
GABA	γ-Aminobutyric acid
GAD67–GFP	Glutamic acid decarboxylase 67–GFP
GFP	Green fluorescent protein
HP	hippocampus
LH	Lateral hypothalamus
mlf	Medial longitudinal fasciculus
NAC	Nucleus accumbens
NAcC	nucleus accumbens core
NAcSh	nucleus accumbens shell
PFC	Prefrontal cortex
TPOH	Tryptophan hydroxylase
xcsp	decussation of the superior cerebral peduncle

MATERIALS AND METHODS

Animals

A total of 22 mice were used in this study. GAD67–GFP mice previously generated (Tamamaki et al., 2003) were bred at the animal facility at the Children's Hospital Boston. The phenotype of each mouse was identified by illuminating mice at postnatal day 1 or 2 with blue light to detect green fluorescence in heterozygotic mice as previously described (Tamamaki et al., 2003). Mice were maintained on a 12-hour light/dark cycle with food and water ad libitum. All procedures were approved by the Institutional Care and Use Committee at Children's Hospital and were consistent with the National Institutes of Health Guide for the Care and Use of Laboratory Animals.

Surgery

Mice (20–50 g; 4–6 weeks old) were anesthetized with 2–2.5 % isoflurane in air mixture administered through a nose cone, and placed in a stereotaxic apparatus. Throughout the surgery, anesthesia was maintained by 1.5–2 % isoflurane through a nose cone, and body temperature was maintained by using a heating pad. The skin was cut along the midline above bregma, and a hole was drilled on the dorsal skull above the target regions. Four percent FG (80014; Biotium, Hayward, CA), a retrograde tract tracer, was manually injected via a 1-μl Hamilton syringe (25s gauge; #7001; Hamilton, Reno, NV) into one of the three brain regions at the following coordinates: PFC (anterior–posterior [AP], +1.7 mm; medial–lateral [ML], +0.2 mm; dorsoventral [DV], −1.7 mm relative to bregma); NAC (AP, +1.4 mm; ML, +1.2 mm; DV, −3.5 mm relative to bregma); and LH (AP, −0.9 mm; ML, +1.0 mm; DV, −4.5 mm relative to bregma). These coordinates were chosen according to *The Mouse Brain in Stereotaxic Coordinates* (Paxinos and Franklin, 2001). Each injection (0.05–0.07 μl) was made over a 3-minute period, and the syringe was left at the injection site for an additional 3 minutes to allow for diffusion of the tracer. After the injection was completed, the syringe was retracted from the brain, and the incisions were sutured. Animals were kept on heating pads until awake, and then returned to their home cage for recovery.

Tissue preparation

Approximately 6–7 days following surgery, mice were deeply anesthetized with an overdose of sodium pentobarbital (50 mg/kg, i.p.). Transcardial perfusion was made with 4% paraformaldehyde in normal saline. Brains were removed, placed in 4% paraformaldehyde for 24 hours, and cryoprotected in 30% sucrose in 0.1 M phosphate buffer for at least 2 days. Cryoprotected brains were then frozen and sectioned in the coronal plane by using a freezing microtome, and 40-μm free-floating cryosections were further processed.

TABLE 1.
Primary antibodies

Antigen	Immunogen	Manufacturer	Dilution
Green fluorescent protein (GFP)	Purified recombinant GFP	Aves Labs (Tigard, OR), chicken polyclonal, GFP-1020	1:500
Fluoro-gold (FG)	Hydroxystilbamidine	Millipore (Billerica, MA), rabbit polyclonal, AB153	1:2000
Tryptophan hydroxylase (TPOH)	Recombinant rabbit tryptophan hydroxylase, isolated as inclusion bodies from E. coli	Millipore {Billerica, MA), sheep polyclonal, AB1541	1:5000

Immunofluorescence labeling

In order to examine the distribution of GAD67–GFP neurons with respect to 5-HT neurons in the DR, double immunolabeling of GFP and tryptophan hydroxylase (TPOH), an enzyme involved in the synthesis of 5-HT, was conducted. Primary antisera were diluted in 0.1 M phosphate-buffered saline (PBS) with 0.3% Triton X-100, 0.04% bovine serum albumin, and 0.1% sodium azide. Free-floating sections were incubated with a chicken polyclonal anti-GFP antibody (1:500; GFP-1020; Aves Labs, Tigard, OR) and a sheep polyclonal anti-TPOH (1:5000; AB1541; Millipore, Billerica, MA) primary antibody overnight at room temperature. After rinsing in 0.1 M PBS three times, sections were incubated with CY2-conjugated donkey anti-chicken, and CY5-conjugated donkey anti-sheep secondary antibodies (Jackson ImmunoResearch, West Grove, PA) for 90 minutes at room temperature.

Although GFP and FG are fluorescent, GFP and FG were double immunolabeled in order to improve detection. This was done by incubating free-floating sections with a chicken polyclonal anti-GFP antibody and a rabbit polyclonal anti-FG antibody (1:2,000; AB153; Millipore) for 2 days at 4°C. Following three rinses in 0.1 M PBS, primary antisera were detected by using CY2-conjugated donkey anti-chicken and CY3-conjugated donkey anti-rabbit secondary antibodies (Jackson ImmunoResearch). Sections were then washed in 0.1 M PBS, and mounted onto glass slides and coverslipped with 90% glycerol-containing mounting media.

Antibody characterization

The primary antibodies used are listed in Table 1.

1. Chicken anti-GFP (GFP-1020; Aves Labs). The antibody was raised in chickens that were immunized with purified recombinant GFP emulsified in Freund's adjuvant (Aves Labs datasheet). Tan and colleagues (2008) reported that the antibody stains virally induced GFP-expressing neurons in adult rats. The specificity of the antibody was previously confirmed by the lack of staining in rat brain tissues not infected with the virus (Tan et al., 2010).
2. Sheep anti-TPOH polyclonal antibody (AB1541; Millipore). The antibody was affinity purified, and was raised against a recombinant rabbit TPOH (Millipore datasheet). It recognizes tryptophan hydroxylase (55 kDa) on western blots from rat DR (Millipore datasheet). A partial cross-reactivity with tyrosine hydroxylase has been reported (manufacturer's description; Kaufling et al., 2009).
3. Rabbit anti-FG polyclonal antibody (AB153; Millipore). Hydroxystilbamidine was used as the immunogen to produce this antibody (manufacturer's description). Kaufling et al. (2009) showed that this antibody specifically identifies neurons containing the retrograde tract tracer in rats that received stereotaxic injection of FG. No immunolabeling was detected in animals not injected with FG (Ito et al., 2007; Kaufling et al., 2009).

Microscopy and image processing

Sections were imaged on an inverted spinning-disc confocal microscope (Olympus IX81-DSU, Tokyo, Japan) by using a Hamamatsu Orca ER camera with conventional mercury bulb illumination and Slidebook software (3i). The regions of interest were illuminated for each fluorophore, and photographed. Neurons that were double immunolabeled for GFP and FG were enumerated by visualizing individual and merged images of each fluorophore. The resulting images were exported to Adobe Photoshop 4.0 software (Adobe Systems, San Jose, CA) to further adjust size, brightness by using 'adjustment brightness,' and contrast by using 'adjustment curves' for presentation in the figures.

Data analysis

The number of single-labeled FG-containing neurons and double-labeled neurons expressing both GFP and FG was counted in seven subregions in the DR (Fig. 1C,F,I). The DR was divided along the anterior–posterior axis into thirds based on the organization of 5-HT neurons: rostral level was from −4.16 to −4.24 mm, middle level was

from −4.36 to −4.84 mm, and caudal level was from −4.96 to −5.20 mm relative to Bregma (Paxinos & Franklin, 2001). The rostral and middle levels were further divided into dorsal, ventral, and medial longitudinal fasciculus (mlf) zones, and the caudal level was divided into dorsal and ventral subdivisions. On average, three fields were photographed for each region of interest in each mouse at 10, 20, and 60× magnification. For each

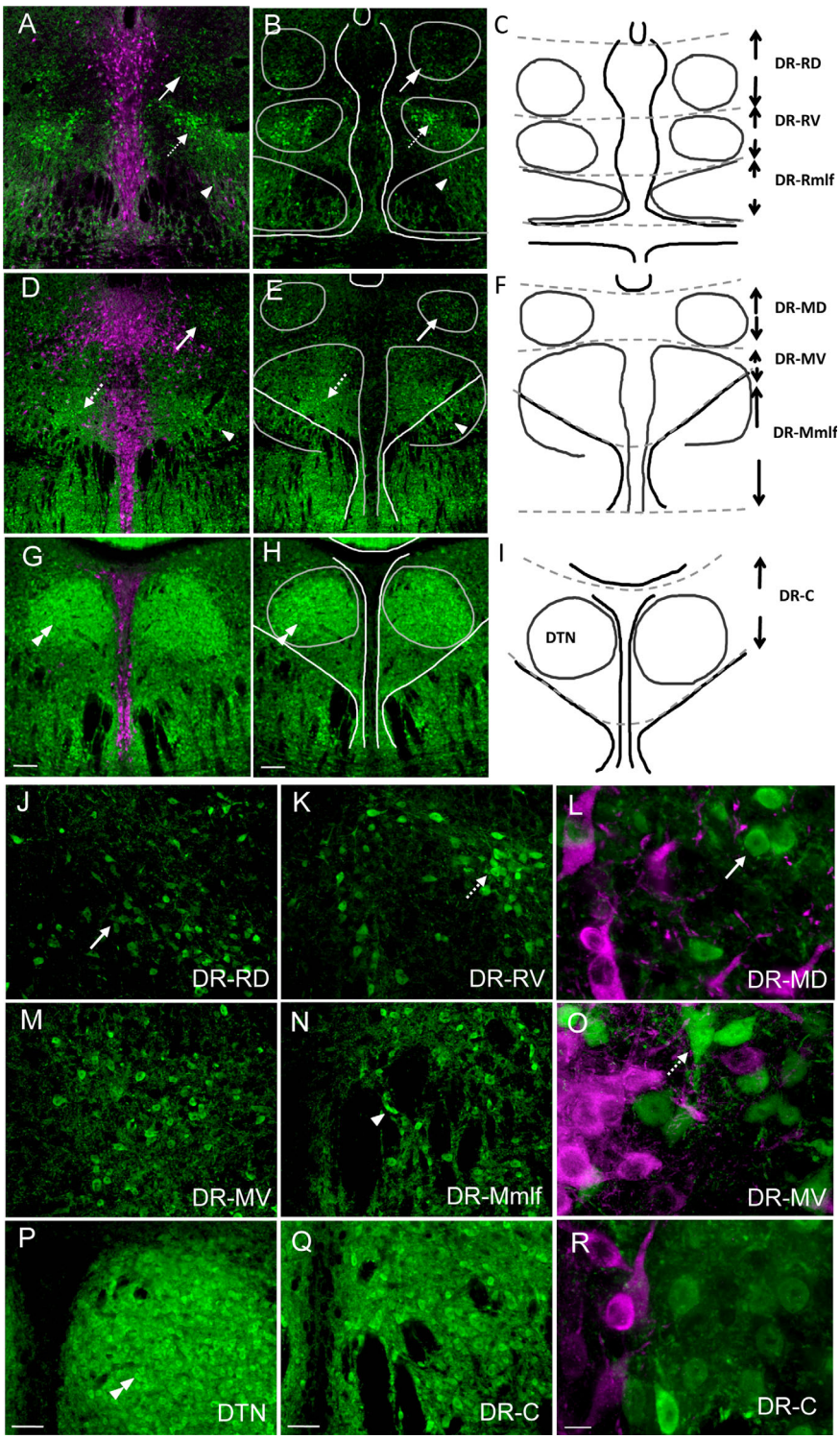

Figure 1

mouse, every fourth section was analyzed, representing two to three sections per region of interest. The location of neurons containing FG or both FG and GFP in the regions of interest was drawn by using Adobe Photoshop 4.0 software.

The percentage of neurons double-labeled with both GFP and FG overall or per section/per subdivision was calculated by dividing the number of neurons with both GFP and FG by the total number of neurons with only FG immunolabeling and FG with GFP immunolabeling. Group mean percentage and standard error of the mean percentage were calculated overall or for each subregion, accordingly. Repeated measures analysis of variance (ANOVA; SPSS 14.0; Chicago, IL) was used to analyze each subregion with REGION as a within-subject factor and FG injection site (PFC, NAC, and LH) as a between-subject factor. A significant interaction effect was followed by one-way ANOVA, and post hoc Tukey's honestly significant difference (HSD) test with a threshold for significance of $P < 0.05$ where appropriate.

RESULTS

GAD67–GFP distribution and organization in the DR

The organization and projections of 5-HT neurons are known to vary with their location within the DR (Vasudeva et al., 2011; Waselus et al., 2011). Therefore, we studied the distribution of GAD67–GFP neurons with respect to 5-HT neurons to develop a scheme to describe the location of projecting neurons within the DR. GAD67–GFP neurons (green) were primarily located lateral to midline TPOH-containing neurons (magenta) at all levels (Fig. 1A,D,G), and only an occasional neuron was double immunolabeled for both GFP and TPOH, consistent with previous observations of the mouse ventral periaqueductal gray (Brown et al., 2008; Fu et al., 2010). There were differences in the distribution of GAD67–GFP neurons along the rostral–caudal axis (Fig. 1A,D,G) in that loosely organized groups of neurons were visible within the rostral and middle third of the DR, and these groups differed from those located within the caudal third of the nucleus.

Similarly in both the rostral (Fig. 1A,B) and middle (Fig. 1D,E) third of the DR, dorsal (DR-RD and DR-MD) and ventral (DR-RV and DR-MV) clusters of GAD67–GFP neurons were noted. The dorsally located GAD67–GFP neurons tended to have a small diameter (approximately 10 μm) and were dimly immunolabeled for GFP (Fig. 1J,L). More ventrally located GAD67–GFP neurons were variable in size (up to approximately 20 μm) and included more intensely GFP-immunolabeled neurons (Fig. 1K,M,O). Continuing ventrally, GAD67–GFP neurons were not bounded by the mlf, but were found scattered within and ventral to these fiber tracts (Fig. 1N). At the caudal pole of the DR (Fig. 1G,H), this pattern shifted and most GAD67–GFP neurons were densely packed within the dorsal tegmental nuclei of Gudden (DTN; Fig. 1P), with a few remaining GAD67–GFP neurons dispersed in the vicinity (DR-C; Fig. 1Q,R). In our subsequent analysis, we mapped the location of GAD67–GFP neurons with retrograde tract tracer with respect to these distribution trends.

PFC-projecting neurons

FG microinjections into PFC were made in seven animals 1 week prior to perfusion. Three animals died during surgeries, and thus were not further processed. Another subject was also omitted from data analysis due to misplacement of the FG injection. In the remaining three mice analyzed, the injection site was centered within both the prelimbic and infralimbic cortices. (Fig. 2A shows a representative case.) Although the injections

Figure 1. Distribution of GFP-expressing GAD67 neurons (green) with respect to TPOH-stained neurons (magenta) in the DR. **A,B**: In the rostral third of the DR, a dorsal cluster of neurons dimly immunolabeled for GFP (arrows) and a ventral, more intensely labeled group (dashed arrows) are present. GAD67–GFP-immunolabeled neurons continue ventrally, interspersed within fiber bundles of the mlf (arrowhead). **C**: Reference schematic drawing showing landmarks used to plot the location of projecting GAD67–GFP neurons, with their abbreviations: DR-RD, rostral dorsal DR; DR-RV, rostral ventral DR; DR-Rmlf, rostral medial longitudinal fasciculus. **D,E**: In sections passing through the middle third of the DR, again dorsal (arrows) and ventral (dashed arrows) groups of GAD67–GFP neurons are seen, as well as those extending through the mlf (arrowhead). **F**: Reference schematic showing the middle dorsal (DR-MD), middle ventral (DR-MV), and middle medial longitudinal fasciculus (DR-Mmlf). **G,H**: In the caudal third of the DR, packed GAD67–GFP neurons are visible within the dorsal tegmental nucleus of Gudden (DTN, double arrowhead), as well as dispersed in the surrounding neuropil. **I**: Reference schematic drawing. **J**: GAD67-GFP neurons in the rostral and dorsal DR typically have small cell bodies (arrow). **K**: Rostral and ventral, GAD67–GFP neurons can be more intensely labeled and are larger (dashed arrow). **L**: Higher magnification of round, GAD67–GFP neurons (arrow) located dorsally. **M**: Many GAD67–GFP neurons located mid-ventral. **N**: GAD67–GFP neurons interspersed between fiber bundles (arrowhead). **O**: GAD67–GFP neurons (dashed arrow) with variable morphology in mid-ventral (DR-MV). **P**: GAD67–GFP neurons packed in the DTN (double arrowhead). **Q**: GAD67–GFP neurons dispersed caudally in the DR. **R**: Higher magnification of neurons located in the caudal DR. Scale bar = 100 μm in G (applies to A,D,G) and H (applies to B,E,H); 50 μm in P (applies to J,M,P) and Q (applies to K,N,Q); 10 μm in R (applies to L,O,R). [Color figure can be viewed in the online issue, which is available at wileyonlinelibrary.com.]

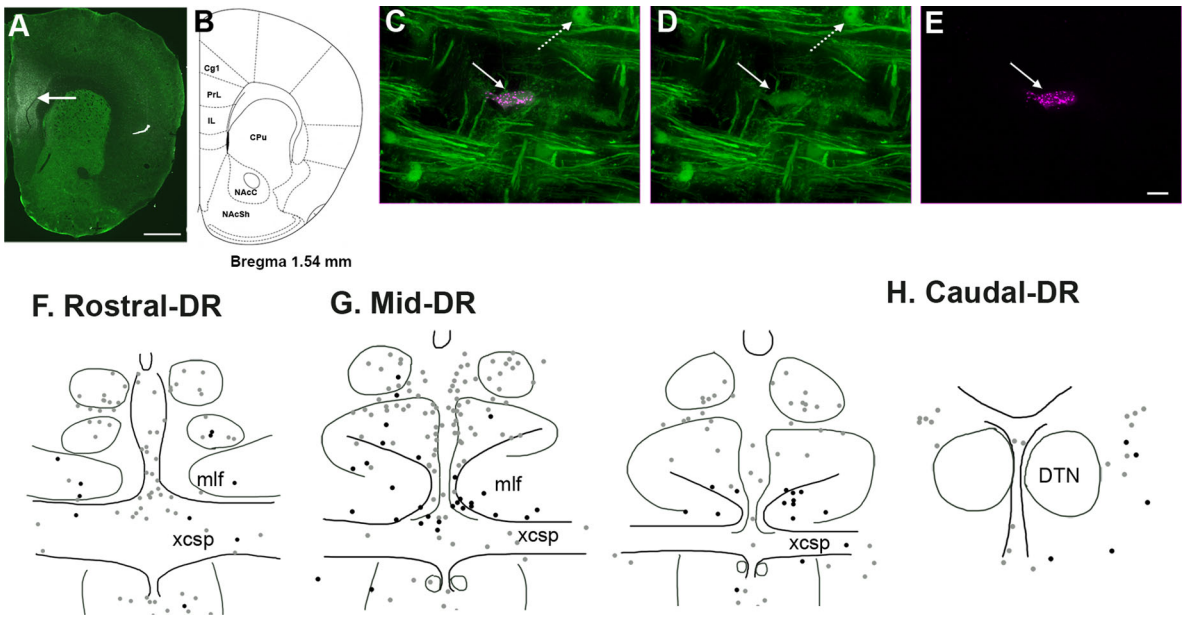

Figure 2. Location of neurons projecting to the prefrontal cortex (PFC), with and without GAD67–GFP in the DR. **A,B**: A representative image of FG injection in the PFC (arrow) with corresponding bran atlas section adapted from Paxinos and Franklin (2001). Drug diffusion was restricted within the prelimbic (PrL) and infralimbic cortex (IL). **C–E**: Immunofluorescence labeling for GFP (green) and FG (magenta) shows a double-labeled GAD67–GFP neurons (straight arrow) retrogradely labeled from the PFC. In addition, a neuron solely labeled for GFP is visible (dashed arrow) in the mlf region of the DR. D and E show immunolabeling for GFP and FG, respectively; they are merged in C. **F–H**: Schematic illustrations of brain sections showing distribution of PFC-projecting neurons that are either GAD67–GFP (black dots) or non-GAD67–GFP (gray dots) at the rostral, middle, and caudal levels of the DR. Abbreviations: Cg1, cingulate cortex; CPu, caudate putamen; DTN, the dorsal tegmental nuclei of Gudden; mlf, medial longitudinal fasciculus; NAcC, nucleus accumbens core; NAcSh, nucleus accumbens shell; xcsp, decussation of the superior cerebral peduncle. For other abbreviations, see list. Scale bar = 1 mm in A; 20 micrometer in E (applies to C–E). [Color figure can be viewed in the online issue, which is available at wileyonlinelibrary.com.]

were restricted to the medial prefrontal cortex (mPFC), a possibility of slight diffusion into surrounding areas including the dorsal peduncular cortex and cingulate cortex cannot be excluded. Although the needle tract was identified, surrounding necrosis due to the FG injection was not detected.

In sum, PFC-projecting neurons in the DR were enriched in the rostral and middle third of the DR, and overall 16% of the total number of projecting neurons contained GAD67–GFP immunolabeling. The distribution of projecting neurons with (black dots in Fig. 2F–H) and without GAD67–GFP (gray dots in Fig. 2F–H) differed. GAD67–GFP neurons that projected to the PFC were preferentially interspersed between dense fibers of passage in the mlf (Fig. 1N), and as such were located ventral to many non-GAD67–GFP neurons projecting to the PFC (Fig. 2G). Expressed as a percentage of the total number of retrogradely labeled neurons in each subdivision, the highest percentage of PFC-projecting neurons that were GAD67–GFP was found in the DR-Mmlf (38.1 ± 15%) and in the DR-Rmlf (21.7 ± 8.8%; Table 2). Overall, there were few retrogradely labeled neurons, with or without GAD67–GFP in the caudal third of the DR (Fig. 2H).

NAC-projecting neurons

A total of nine mice received unilateral FG microinjection into the NAC, and three of them were included in the data analysis. In the excluded subjects, FG spread either dorsally or caudally from the NAC, or no FG-labeled cells were detected in the NAC. In the three animals that were analyzed, the FG injection site encompassed both the core and shell regions of the NAC (Fig. 3A).

GAD67–GFP neurons constituted a similar fraction of the neurons projecting to the PFC and NAC (16% overall) and had a partially overlapping distribution. The major difference between GAD67–GFP neurons projecting to the NAC versus the PFC was that NAC-projecting GAD67–GFP neurons were also prevalent within the ventral subdivision of the middle third of the DR, i.e., dorsal to the location of many PFC-projecting GAD67–GFP neurons. GAD67–GFP neurons that were double labeled with GFP

and FG were most commonly found in the middle third of the DR, particularly in the DR-MV and DR-Mmlf (Fig. 3G), where they accounted for almost a third of NAC-projecting neurons in each region: DR-MV (27.7 ± 2.1%) and DR-Mmlf (29.4 ± 3.9%) (Table 2). GAD67–GFP neurons projecting to the NAC in the caudal DR were rarely identified (Fig. 3H).

TABLE 2.

Average number (mean percentage) of FG-stained forebrain-projecting GABA neurons in DR

	PFC	NAC	LH
DR-RD	0.8 ± 0.4	3.5 ± 1.9	13 ± 3
	(4.4 ± 1.7 %)	(5.6 ± 4.7 %)	(20.2 ± 2.4 %)
DR-RV	4.3 ± 1.7	0.3 ± 0.3	7.3 ± 5.4
	(15.8 ± 6.4%)	(2 ± 1.9%)	(20.7 ± 13.4%)
DR-Rmlf	7.5 ± 4.8	2.2 ± 1.1	15 ± 4.6
	(21.7 ± 8.8%)	(7.3 ± 3.8 %)	(45 ±15.9%)
DR-MD	4 ± 2	24 ± 7.1	30 ± 1.2
	(6.2 ± 3.2 %)	(12.6 ± 2.7%)	(23.2 ± 1.1%)
DR-MV	4.7 ± 2.6	27 ± 8.6	40 ± 8.5
	(8.1 ± 5.8%)	(27.7 ± 2.1 %)	(26.8 ± 4.3%)
DR-Mmlf	13 ± 5	11 ± 5	55 ± 3
	(38.1 ± 15%)	(29.4 ± 3.9 %)	(54 ± 8.4%)
DR-C	1.8 ± 0.8	1.1 ± 1.1	19.9 ± 6.1
	(9.8 ± 5.8 %)	(5 ± 4.9 %)	(51.2 ± 8.4%)

For abbreviations, see list.

LH-projecting neurons

A total of six mice received unilateral FG microinjection into LH. Two subjects were not included in the analysis as FG extended too much into surrounding regions, and one subject was excluded due to failure to detect FG in the LH. Although the injection was localized in the LH (Fig. 4A), some FG may have extended into the anterior hypothalamic area.

LH-projecting neurons with (black dots) and without GAD67–GFP (gray dots) were widely distributed throughout the DR along the whole anterior–posterior axis (Fig. 4F–H), and outnumbered both PFC- and NAC-projecting neurons in the DR. In addition, GAD67–GFP neurons constituted a greater fraction of the total number of projecting neurons (36% on average). GAD67–GFP neurons projecting to the LH (black dots) were present in the highest density in the DR-Rmlf (Fig. 4F), DR-Mmlf (Fig. 4G), and DR-C (Fig. 4H). Mean percentages of the LH-projecting GAD67–GFP neurons in these three regions were as follows: 54 ± 8.4% in DR-Mmlf; 51.2 ± 8.4% in DR-C; and

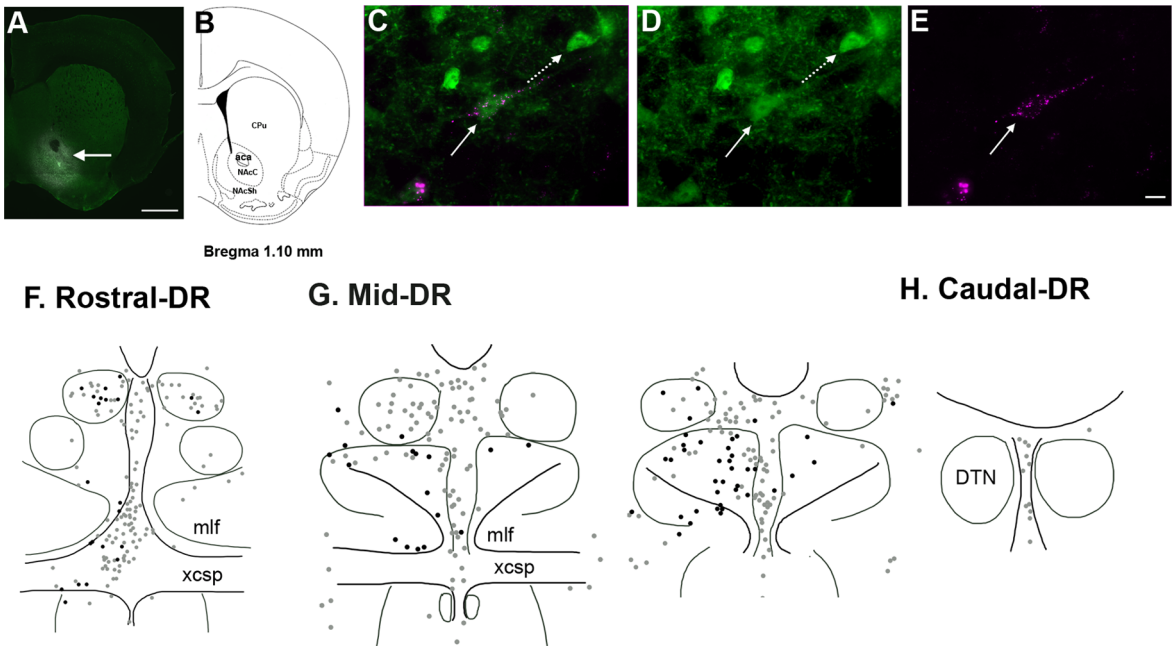

Figure 3. Distribution of DR neurons projecting to the nucleus accumbens (NAC), with and without GAD67–GFP. **A,B**: A representative image showing FG injection in the NAC with corresponding brain atlas section adapted from Paxinos and Franklin (2001). FG diffused into both the core (NAcC) and shell (NAcSh) regions of the NAC (arrow) surrounding the anterior commissure (aca). **C–E**: An example of NAC-projecting GAD67–GFP neurons (straight arrow) double labeled for GFP (green) and FG (magenta). An adjacent GAD67–GFP neuron (dashed arrow) lacks immunolabeling for FG. Immunolabeling for GFP and FG observed individually in D and E, respectively. **F–H**: Schematic illustrations of the distribution of NAC-projecting neurons that contain GAD67–GFP (black dots) or lack GAD67–GFP (gray dots) in the rostral, middle, and caudal DR. For abbreviations, see list. Scale bar = 1 mm in A; 20 micrometer in E (applies to C–E). [Color figure can be viewed in the online issue, which is available at wileyonlinelibrary.com.]

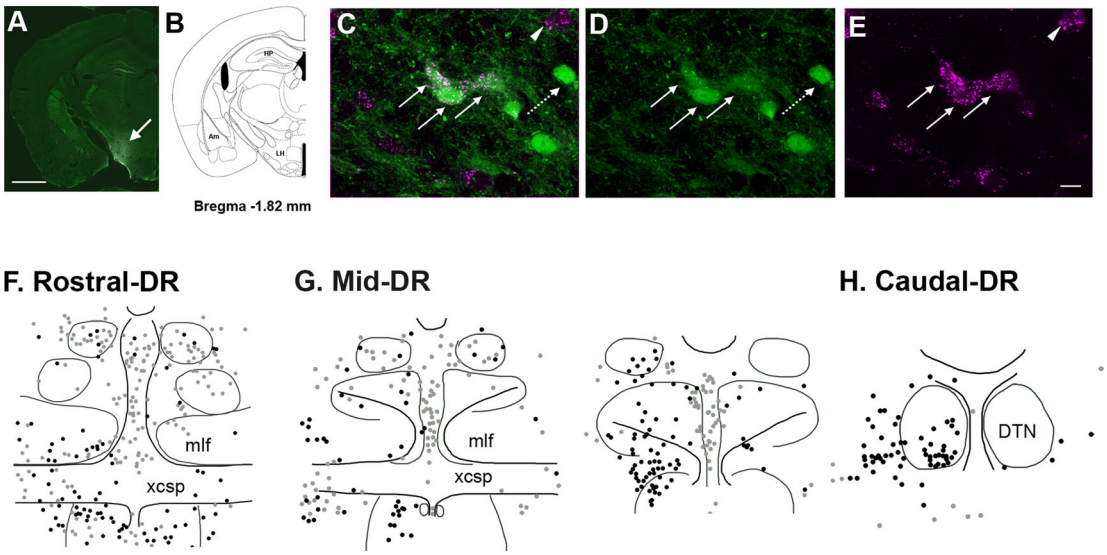

Figure 4. Distribution of neurons projecting to the lateral hypothalamus (LH) with and without GAD67–GFP. **A,B**: FG diffusion was restricted in the LH (arrow) as shown in the representative image with corresponding brain atlas section adapted from Paxinos and Franklin (2001). **C–E**: GAD67–GFP neurons projecting to the LH (straight arrows) were double labeled with both GFP (green) and FG (magenta), whereas other GAD67–GFP neurons not projecting to the LH (dashed arrow) are labeled with GFP only. A neuron projecting to the LH lacking GAD67–GFP (arrowhead) is also visible. **F–H**: Schematic illustration showing the locations of LH-projecting GAD67–GFP (black dots) and non-GAD67–GFP neurons (gray dots) in the rostral, middle, and caudal levels of the DR, respectively. Abbreviations: Am, amygdala; HP, hippocampus; LH, lateral hypothalamus. For other abbreviations, see list. Scale bar = 1 mm in A; 20 micrometer in E (applies to C–E). [Color figure can be viewed in the online issue, which is available at wileyonlinelibrary.com.]

45 ± 15.9% in DR-Rmlf (Table 2). Notably, unlike the other GAD67–GFP neurons projecting to either the PFC or NAC, LH-projecting GAD67–GFP neurons were densely distributed at the caudal level including the ventral part of the DTN (Fig. 4H).

Mean percentage of forebrain-projecting GAD67–GFP neurons in each subdivision in the DR

There were region-specific differences in the proportion of GAD67–GFP neurons projecting to the three forebrain target regions examined (Fig. 5). Repeated measures ANOVA revealed significant main effects of REGION within the DR ($F(7,14) = 5.89$, $P < 0.01$), FG injection site ($F(2,6) = 23.12$, $P < 0.01$), and a significant interaction between the two factors ($F(14,42) = 1.98$, $P < 0.05$). Further simpler test using one-way ANOVA showed significant group difference among the three target injection sites in the DR-RD ($F(2, 6) = 7.92$, $P < 0.05$), DR-MD ($F(2,6) = 11.93$, $P < 0.01$), DR-MV ($F(2,6) = 6.44$, $P < 0.05$), and DR-C ($F(2,6) = 14.80$, $P < 0.01$). Post hoc Tukey's HSD test revealed that the mean percentage of GAD67–GFP neurons projecting to the LH was significantly higher than those projecting to either the PFC or NAC in the DR-RD, and DR-C ($P < 0.05$). In the DR-MD and DR-MV, the mean percentage of GAD67–GFP neurons projecting to the PFC was significantly lower than that projecting to the LH and NAC, respectively (Fig. 5).

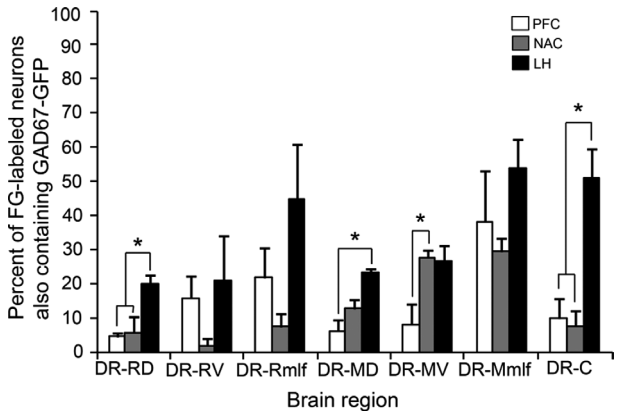

Figure 5. Mean percentage of the total numbers of neurons projecting to each target region that were double immunolabeled for GAD67–GFP, calculated for each subdivision of the DR examined. Mean percentage of GAD67–GFP neurons in each subdivision projecting to the PFC, NAC, or LH are denoted in white, gray, and black bars, respectively. Asterisks denote significant group differences. For abbreviations, see list.

DISCUSSION

GAD67–GFP neurons are located lateral to midline 5-HT neurons in the DR and appear organized in loose

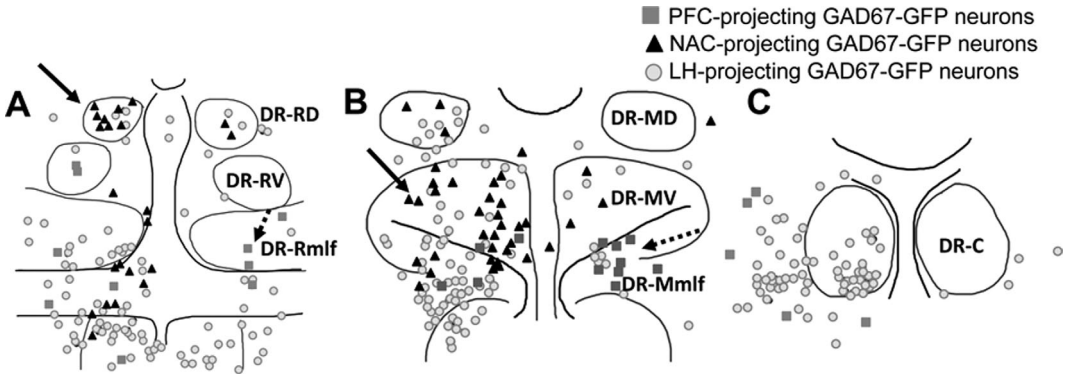

Figure 6. Schematic illustrations showing the locations of GAD67–GFP neurons projecting to each target region examined at the rostral (**A**), mid (**B**), and caudal (**C**) levels of the DR. Within both the rostral (A) and middle third of the DR (B), NAC-projecting GAD67–GFP neurons (black triangles, arrows) tended to be located dorsal to PFC-projecting GAD67–GFP neurons (dark gray squares, dashed arrows) that were mostly located in the mlf region. LH-projecting GAD67–GFP neurons (light gray circles) were distributed throughout the DR subdivisions. At the caudal level (C), GAD67–GFP neurons primarily projected to the LH. For abbreviations, see list.

clusters along the dorsoventral axis. Depending on their location, GAD67–GFP neurons also displayed trends for selective projections to the forebrain. The retrograde tract-tracing findings revealed that the three target regions are innervated by populations of GAD67–GFP neurons from partially overlapping regions within the DR: the PFC was mostly innervated by GAD67–GFP neurons, particularly ventral, intermingling with the mlf at both the rostral and mid-levels of the DR (DR-Rmlf and DR-Mmlf); the NAC received projections primarily from GAD67–GFP neurons in the same and slightly dorsal locations (DR-MV and DR-Mmlf); and the LH was the most densely innervated region by GAD67–GFP neurons that were distributed throughout the DR subdivisions, but particularly at DR-Rmlf, DR-Mmlf, and DR-C. These results indicate that a notable minority of the ascending projections from the DR to the forebrain arise from GABAergic neurons.

Methodological considerations

The retrograde tract tracer FG has been widely used to study neuronal projections in many brain areas (Petrovich et al., 2005; Mascagni and McDonald, 2009; Bubar et al., 2011). Due to the history of FG use, the technical limitations are well established, and contribute to the potential for both false-positive and false-negative error. False-positive error may be created by the spread of FG to neighboring areas as well as the potential for uptake by fibers of passage, particularly when large injection volumes are used and tissue damage is visible at the site of injection. False-negative error leading to the underdetection of projecting neurons is also possible. Incomplete filling of the target area with FG may cause underdetection. In addition, FG may have negative effects on translation in neurons that reduce the ability to detect other markers within the same cells (Franklin and Druhan, 2000). This later effect is also associated with large injection volumes and neurotoxicity at the site of injection.

In the GAD67–GFP mouse line we used, GFP is knocked into the GAD67 locus, such that it is under the control of the same proximal and distal transcriptional regulatory elements as endogenous GAD67 and therefore should have high-fidelity expression in these neurons. Indeed, using the same mouse line, previous studies of GFP expression in the mesencephalon have reported >96% concordance between GFP-containing neurons and those that were immunolabeled for GABA (Brown et al., 2008). GAD67–GFP neurons were found not only in the DR and adjacent periaqueductal gray, but also within the fiber bundles of the mlf and ventral locations, consistent with the previous observations (Brown et al., 2008; Fu et al., 2010). This is consistent with the observation that the mlf does not mark a functional boundary within this region (Holstege, 1991).

PFC-projecting GAD67–GFP neurons in the DR

The rostral and middle third of the DR is known to provide a substantial projection to the PFC (Sarter and Markowitsch, 1984; Waterhouse et al., 1986; Vertes, 1991), and our results indicate that GAD67–GFP neurons contribute to this projection. Among the retrogradely labeled DR neurons projecting to the PFC, 16% were identified as GAD67–GFP neurons. In the rat, studies using anterograde tract tracing have suggested that the PFC projection from the DR almost entirely arises from 5-HT neurons (Kosofsky and Molliver, 1987; Halberstadt and Balaban, 2008). However, retrograde tract-tracing studies have suggested a greater participation of non–5-HT neurons in this pathway (Van Bockstaele et al., 1993). These observations may be resolved, at least in part, by the extreme ventral location of GAD67–GFP neurons projecting to the

PFC from the DR, that is, interspersed within the mlf at both the rostral and middle levels of the DR (Fig. 2F–H). Therefore, these neurons could be underdetected by anterograde studies with more restricted injection sites. The dual GABAergic and 5-HT nature of the projection from the DR to the PFC is consistent with previous electrophysiology showing that electrical stimulation of DR produces a short latency inhibition of pyramidal neurons in the medial PFC through both GABAergic and 5-HT mechanisms (Puig et al., 2005).

NAC-projecting GAD67–GFP neurons in the DR

GAD67–GFP neurons also made a contribution of DR projections to the NAC, constituting 16% of the DR neurons projecting to this area. When detected, GAD67–GFP NAC-projecting neurons were preferentially located in the ventral subdivision of the middle third of the DR, overlapping and slightly dorsal to the location of most GAD67–GFP neurons projecting to the PFC. 5-HT is thought to presynaptically facilitate dopamine release in the NAC, with the potential to influence motivated behaviors (De Deurwaerdère et al., 1998). Although the effect of DR stimulation appears largely dependent on 5-HT neurotransmission (De Deurwaerdère et al., 1998), previous retrograde tract-tracing studies in rats suggested the possibility of a non–5-HT projection to the NAC (Van Bockstaele et al., 1993; Chang et al., 2011). Taken together, these data would support the contribution of DR GABA neurons to the ascending projection to the NAC; however, the functional role of this pathway remains to be established.

LH-projecting GAD67–GFP neurons in the DR

Among the three forebrain-target regions examined in this study, retrograde tract tracing from the LH identified the greatest number of GAD67–GFP and non-GAD67–GFP neurons within the DR. The total number of FG-stained neurons outnumbered those projecting to either the PFC or NAC in all subdivisions of the DR examined, as did the fractional contribution of GAD67–GFP neurons (36%). This observation is consistent with previous anterograde tract-tracing studies in 5-HT–depleted rats that reported dense projections of non–5-HT neurons from the DR to the LH (Halberstadt and Balaban, 2008). However, we cannot exclude the possibility that the identified neurons in the DR, which either ramify within or pass through the LH, provide collateralized projections to additional forebrain targets, because a large number of ascending tracts from the DR pass through this area (Steinbusch, 1984).

What distinguished GAD67–GFP neurons that project to the LH was their greater distribution to dorsal and caudal areas within the DRN in comparison to GABAergic neurons identified to be projecting to the PFC or NAC (Fig. 6). These included neurons located dorsolateral in the middle DR, in an area that may be analogous to the location of GABAergic neurons that have activated Fos expression after swim stress (Roche et al., 2003), consistent with the role of the LH in stress (Seta et al., 2001). At the caudal pole of the DRN, GABAergic neurons within the DTN were also identified with retrograde tract tracing from the LH. The DTN is known to send GABAergic projections to the lateral mammillary nucleus (Wirtshafter and Stratford, 1993) and has been implicated in generating head-direction information via links to the mammillary nucleus (Bassett et al., 2007). The current data would suggest that the ventral DTN also provides projections to the LH, rostral to the mammillary nucleus, with an unknown functional importance.

CONCLUSIONS

Taken together with previous studies, these data suggest that GABAergic neurons in the DR, similar to VGLUT3 glutamatergic neurons, have the capacity to both influence local network activity and contribute to forebrain output. Therefore, output of the DR may not only vary in its frequency and amplitude of activation, but also in its neurochemical content. Although these data add to the complexity of the DR, they may ultimately contribute to a better understanding of how the DR regulates forebrain function.

Conflict of interest: none.

Role of authors: All authors had full access to all the data in the study and take responsibility for the integrity of the data and the accuracy of the data analysis. Study concept and design: S.J.B., K.G.C. Acquisition of data: S.J.B. Analysis and interpretation of the data: S.J.B., K.G.C. Drafting of the manuscript: S.J.B. Critical revision of the manuscript for important intellectual content: K.G.C. Statistical analysis: S.J.B. Obtained funding: K.G.C. Administrative, technical, and material support: S.J.B. Study supervision: K.G.C.

LITERATURE CITED

Ansorge MS, Hen R, Gingrich JA. 2007. Neurodevelopmental origins of depressive disorders. Curr Opin Pharmacol 7: 8–17.

Bassett JP, Tullman ML, Taube JS. 2007. Lesions of the tegmentomammillary circuit in the head direction system disrupt the head direction signal in the anterior thalamus. J Neurosci 27:7564–7577.

Brown RE, McKenna JT, Winston S, Basheer R, Yanagawa Y, Thakkar MM, McCarley RW. 2008. Characterization of GABAergic neurons in rapid-eye-movement sleep controlling regions of the brainstem reticular formation in GAD67-green fluorescent protein knock-in mice. Eur J Neurosci 27:352–363.

Bubar MJ, Stutz SJ, Cunningham KA. 2011. 5-HT(2C) receptors localize to dopamine and GAD67–GFP neurons in the rat mesoaccumbens pathway. PLoS One 6: :e20508

Chang B, Daniele CA, Gallagher K, Madonia M, Mitchum RD, Barrett L, Vezina P, McGehee DS. 2011. Nicotinic

excitation of serotonergic projections from dorsal raphe to the nucleus accumbens. J Neurophysiol 106:801–808.
Chen L, McKenna JT, Leonard MZ, Yanagawa Y, McCarley RW, Brown RE. 2010. GAD67–GFP knock-in mice have normal sleep-wake patterns and sleep homeostasis. Neuroreport 21:216–220.
De Deurwaerdère P, Stinus L, Spampinato U. 1998. Opposite change of in vivo dopamine release in the rat nucleus accumbens and striatum that follows electrical stimulation of dorsal raphe nucleus: role of 5-HT3 receptors. J Neurosci 18:6528–6538.
Descarries L, Watkins KC, Garcia S, Beaudet A. 1982. The serotonin neurons in nucleus raphe dorsalis of adult rat: a light and electron microscope radioautographic study. J Comp Neurol 207:239–254.
Franklin TR, Druhan JP. 2000. The retrograde tracer fluorogold interferes with the expression of fos-related antigens. J Neurosci Methods 98:1–8.
Fu W, Le Maître E, Fabre V, Bernard JF, David Xu ZQ, Hökfelt T. 2010. Chemical neuroanatomy of the dorsal raphe nucleus and adjacent structures of the mouse brain. J Comp Neurol 518:3464–3494.
Halberstadt AL, Balaban CD. 2008. Selective anterograde tracing of nonserotonergic projections from dorsal raphe nucleus to the basal forebrain and extended amygdala. J Chem Neuroanat 35:317–325.
Hensler JG. 2006. Serotonergic modulation of the limbic system. Neurosci Biobehav Rev 30:203–214.
Hioki H, Nakamura H, Ma YF, Konno M, Hayakawa T, Nakamura KC, Fujiyama F, Kaneko T. 2010. Vesicular glutamate transporter 3-expressing nonserotonergic projection neurons constitute a subregion in the rat midbrain raphe nuclei. J Comp Neurol 518:668–686.
Holstege G. 1991. Descending pathways from the periaqueductal gray and adjacent areas. In: Depaulis A, Bandler R, editors. The midbrain periaqueductal gray matter. New York: Plenum Press. p 239–266.
Ito T, Hioki H, Nakamura K, Tanaka Y, Nakade H, Kaneko T, Iino S, Nojyo Y. 2007. Gamma-aminobutyric acid-containing sympathetic preganglionic neurons in rat thoracic spinal cord send their axons to the superior cervical ganglion. J Comp Neurol 502:113–125.
Kaufling J, Veinante P, Pawlowski SA, Freund-Mercier MJ, Barrot M. 2009. Afferents to the GABAergic tail of the ventral tegmental area in the rat. J Comp Neurol 513:597–621.
Kosofsky BE, Molliver ME. 1987. The serotoninergic innervation of cerebral cortex: different classes of axon terminals arise from dorsal and median raphe nuclei. Synapse 1: 153–168.
Mascagni F, McDonald AJ. 2009. Parvalbumin-immunoreactive neurons and GABAergic neurons of the basal forebrain project to the rat basolateral amygdala. Neuroscience 160: 805–812.
Moore RY. 1981. The anatomy of central serotonin systems in the rat brain. In: Jacobs BL, Gelperin A, editors. Serotonin neurotransmission and behavior. Cambridge, MA; MIT Press. p 35–71.
Neumeister A, Young T, Stastny J. 2004. Implications of genetic research on the role of the serotonin in depression: emphasis on the serotonin type 1A receptor and the serotonin transporter. Psychopharmacology (Berl) 174:512–524.
Paxinos G, Franklin KBJ. 2001. The mouse brain in stereotaxic coordinates, deluxe ed. of the Atlas 2nd ed. San Diego, CA: Academic Press.
Petrovich GD, Holland PC, Gallagher M. 2005. Amygdalar and prefrontal pathways to the lateral hypothalamus are activated by a learned cue that stimulates eating. J Neurosci 25:8295–8302.
Puig MV, Artigas F, Celada P. 2005. Modulation of the activity of pyramidal neurons in rat prefrontal cortex by raphe stimulation in vivo: involvement of serotonin and GABA. Cereb Cortex 15:1–14.
Roche M, Commons KG, Peoples A, Valentino RJ. 2003. Circuitry underlying regulation of the serotonergic system by swim stress. J Neurosci 23:970–977.
Sarter M, Markowitsch HJ. 1984. Collateral innervation of the medial and lateral prefrontal cortex by amygdaloid, thalamic, and brain-stem neurons. J Comp Neurol 224: 445–460.
Seta KA, Jansen HT, Kreitel KD, Lehman M, Behbehani MM. 2001. Cold water swim stress increases the expression of neurotensin mRNA in the lateral hypothalamus and medial preoptic regions of the rat brain. Brain Res Mol Brain Res 86:145–152.
Soiza-Reilly M, Commons KG. 2011a. Quantitative analysis of glutamatergic innervation of the mouse dorsal raphe nucleus using array tomography. J Comp Neurol 519: 3802–3814.
Soiza-Reilly M, Commons KG. 2011b. Glutamatergic drive of the dorsal raphe nucleus. J Chem Neuroanat 41:247–255.
Steinbusch HWM. 1984. Serotonin-immnoreactive neurons and their projections in the CNS. In: Bjorklund A, Hokfelt T, Kuhar MJ, editors. Handbook of chemical neuroanatomy. New York: Elsevier Science Publishers. p 68–121.
Tamamaki N, Yanagawa Y, Tomioka R, Miyazaki J, Obata K, Kaneko T. 2003. Green fluorescent protein expression and colocalization with calretinin, parvalbumin, and somatostatin in the GAD67–GFP knock-in mouse. J Comp Neurol 467:60–79.
Tan W, Janczewski WA, Yang P, Shao XM, Callaway EM, Feldman JL. 2008. Silencing preBötzinger complex somatostatin-expressing neurons induces persistent apnea in awake rat. Nat Neurosci 11:538–540.
Tan W, Pagliardini S, Yang P, Janczewski WA, Feldman JL. 2010. Projections of preBötzinger complex neurons in adult rats. J Comp Neurol 518:1862–1878.
Van Bockstaele EJ, Biswas A, Pickel VM. 1993. Topography of serotonin neurons in the dorsal raphe nucleus that send axon collaterals to the rat prefrontal cortex and nucleus accumbens. Brain Res 624:188–198.
Varga V, Losonczy A, Zemelman BV, Borhegyi Z, Nyiri G, Domonkos A, Hangya B, Holderith N, Magee JC, Freund TF. 2009. Fast synaptic subcortical control of hippocampal circuits. Science 326:449–453.
Vasudeva RK, Lin RC, Simpson KL, Waterhouse BD. 2011. Functional organization of the dorsal raphe efferent system with special consideration of nitrergic cell groups. J Chem Neuroanat 41:281–293.
Vertes RP. 1991. A PHA-L analysis of ascending projections of the dorsal raphe nucleus in the rat. J Comp Neurol 313: 643–668.
Waselus M, Valentino RJ, Van Bockstaele EJ. 2011. Collateralized dorsal raphe nucleus projections: a mechanism for the integration of diverse functions during stress. J Chem Neuroanat 41:266–280.
Waterhouse BD, Mihailoff GA, Baack JC, Woodward DJ. 1986. Topographical distribution of dorsal and median raphe neurons projecting to motor, sensorimotor, and visual cortical areas in the rat. J Comp Neurol 249:460–476, 478–481.
Wirtshafter D, Stratford TR. 1993. Evidence for GABAergic projections from the tegmental nuclei of Gudden to the mammillary body in the rat. Brain Res 630:188–194.